Journal of Solid Mechanics Vol. 9, No. 3 (2017) pp. 608-618

# An Upper Bound Analysis of Sandwich Sheet Rolling Process

H. Haghighat *, P. Saadati

*Mechanical Engineering Department, Razi University, Kermanshah, Iran*

Received 28 June 2017; accepted 24 August 2017

**ABSTRACT**

In this research, flat rolling process of bonded sandwich sheets is investigated by the method of upper bound. A kinematically admissible velocity field is developed for a single layer sheet and is extended into the rolling of the symmetrical sandwich sheets. The internal, shear and frictional power terms are derived and they are used in the upper bound model. Through the analysis, the rolling torque, the roll separating force and the thickness of each layer at the exit of deformation are determined. The validity of the proposed analytical method is discussed by comparing the theoretical predictions with the experimental data found in the literature and by the finite element method. It is shown that the accuracy of the newly developed analytical model is good.



**Keywords:** Flat rolling; Sandwich sheet; Upper bound method.

## 1 INTRODUCTION

FLAT rolling is a continuous metal forming process in which thickness of metal sheet or strip is reduced by passing it between a pair of rotating cylindrical rolls having their axes parallel to one another. The primary purpose in analyzing rolling process is to determine unknown process variables, such as rolling force and torque. In this process, accurate prediction of the required torque and the roll force is a major issue. The problem is especially important in multilayered sheet rolling process. Multilayer sheets, consisting of two or more different material layers, make possibility of combining properties of dissimilar sheet metals.

In the past, a number of investigators have presented mathematical analyses for the flat rolling process of single and multilayered sheet materials. Avitzur and Pachla [1-2] proposed an upper bound approach for the plane strain deformation of a rigid-perfectly plastic sheet material. In that approach the deformation region is divided into a finite number of rigid triangular bodies sliding with respect to each other. Explicit equation are then derived to describe the surfaces of velocity discontinuities, shear boundaries, between the moving rigid zones, the velocity discontinuities and the shear power loses along those surfaces. Based on the upper bound theorem, Hwang et al. [3, 4] proposed their own theoretical models to investigate the deformation behavior of the multilayer sheets in the rolling process. A mathematical model using stream functions and the upper bound method has been proposed by the present authors to investigate the plastic deformation behavior of sheets at the roll gap with the assumption that the bonding is completed after rolling [5, 6]. Martins et al. [7] presented an approach based on a solution resulting from the combination of the upper bound method with the weighted residuals method for analysing plane strain rolling. They assumed that plastic deformation zone, bounded by two planes perpendicular to the symmetry axis and contact surface. Dogruoglu [8] presented a method for constructing kinematically admissible velocity fields, which were necessary in the analysis of the flat rolling process by the upper bound method. It was assumed that the trajectories followed by the material point in the plastic deformation zone could be represented as a one-parameter

*Corresponding author. Tel.: +98 83 34274530; Fax: +98 83 34274542.
*E-mail address: hhaghighat@razi.ac.ir* (H.Haghighat).

family of curves in Cartesian coordinates. In the analysis, he assumed that one of the entry or exit surfaces to the deformation zone was plane perpendicular to the symmetry axis. Maleki et al. [9] developed an analytical model based on upper bound method for cold rolling of bimetal strips. The deformation region divided into six rigid zones and for constricting each deformation zone assumed a large number of assumptions. Zhang et al. [10] proposed a three-dimensional velocity field for plate rolling by global weighted method based on assuming cross-sections remain plane and vertical lines remain straight.

In this research, we begin in the next section with explaining of the kinematically admissible velocity field for the flat rolling of single layer sheet and discussing of some mathematical aspects involved in this method in details. In section 3, the proposed kinematically admissible velocity field is extended to rolling of symmetrical sandwich sheets bonded before rolling and the internal, shear and frictional power terms are derived. Section 4 is devoted to demonstrate the validity of this method. The analytical rolling torque and roll separating force are compared with the experimental data of Ref. [11]. Finally, the FEM simulation on the rolling of single layer and sandwich sheets are conducted and a further discussion and comparison with FEM simulation results are presented.

## 2 ROLLING OF THE SINGLE LAYER SHEET

### *2.1 Geometric shape of deformation zones*

Fig. 1 shows the flat rolling process parameters in a schematic diagram. Due to symmetry of the deformation, only the upper half of the process is needed for the analysis. The material starts as a sheet of thickness $2t_o$ and is rolled into a sheet product of thickness $2t_f$ . In Fig. 1, $R$ denotes the roll radius. To analyze the process by using the upper bound method, the material under deformation is divided into three zones, as shown in Fig. 1. In zones I and III the material moves rigidly parallel to the symmetry axis with velocities $v_o$ and $v_f$ , respectively.

Since it is assumed that there is no change in width (plane strain problem) and because of volume constancy, the following relation holds

$$v_o t_o = v_f t_f , \quad \frac{v_o}{v_f} = \frac{t_f}{t_o} \tag{1}$$

Therefore, the speed of the sheet material steadily increases as it moves through the rolls. Zone II is the deformation zone and is surrounded by two cylindrical velocity discontinuity surfaces $S_1$ and $S_2$ as well as the contact surface $S_3$ . The mathematical equations for radial positions of surfaces $S_1$ and $S_2$ are given by

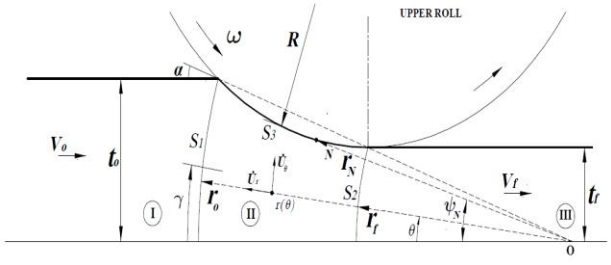


**Fig.1**
Schematic diagram of half-section of the flat rolling process. The cylindrical coordinate system and deformation zones are shown.

$$r_o = \frac{t_o}{\sin\alpha}, \quad r_f = \frac{t_f}{\sin\alpha} \tag{2}$$

The arc of contact, which is labeled as $\psi(r)$ in Fig. 1, is given in the cylindrical coordinate system, $(r,\theta,z)$ , where $\psi(r)$ is the angular position of the contact arc as a function of the radial distance from the origin. The origin of cylindrical coordinate system is located at point *O* which is defined by the intersection of the symmetry axis with a line at angle $\alpha$ that goes through the points where the contact arc begins and the exit point. The equation, which relates the processing parameters to the die angle $\alpha$ , is

$$\alpha = \tan^{-1} \frac{t_o - t_f}{\sqrt{(t_o - t_f)(2R + t_f - t_o)}} \tag{3}$$

The angular position of the cylindrical surface of the contact as a function of the radial distance from the origin is given by solving the following equation

$$(r\sin\psi - R - t_f)^2 + (r\cos\psi - \frac{t_f}{\tan\alpha})^2 = R^2 \tag{4}$$

*2.2 Velocity field in the deformation zone*

After designing each zone and bounding conditions. In each individual zone, the velocity field and its derivatives should be continuous. The expressions describing the velocity vector in two neighboring zones are not identical, but because of volume constancy, the normal component of velocity across boundaries between two zones should be continuous. Parallel to the surface, velocity discontinuity may exist. The method presented in this study is similar to the method proposed in [16, 17] for constructing kinematically admissible velocity fields for axisymmetric and plane strain problems to analyse the deformation of the material in extrusion.

The velocity component in the radial direction within the deformation zone II, $\dot{U}_r$, can be obtained by assuming volume flow balance. In Fig. 1, the volume flow of material per unit with of the sheet, across the surface $S_1$ at the point $(r_o, \gamma, z)$ in the radial direction is

$$dQ = -v_o \cos\gamma\, r_o\, d\gamma \tag{5}$$

where $\beta$ is an arbitrary angle on cylindrical surface $S_1$. The volume flow of material in the radial direction at the point $(r, \theta, z)$ in the deformation zone II is

$$dQ = \dot{U}_r\, r\, d\theta \tag{6}$$

Equating Eqs. (5) and (6), it follows that

$$\dot{U}_r = -v_o \frac{r_o}{r}\cos\gamma \frac{d\gamma}{d\theta} \tag{7}$$

Assuming proportionality distances from the symmetry axis in the deformation zone, the relationship between angular positions $\gamma$ on $S_1$ and the angular position $\theta$ in deformation zone is given by

$$\frac{\sin\gamma}{\sin\alpha} = \frac{\sin\theta}{\sin\psi} \tag{8}$$

where $\psi$ is the angular position of a point on the roll surface at radial distance $r$ from the origin $O$. Differentiating Eq. (8) yields

$$\cos\gamma \frac{d\gamma}{d\theta} = \sin\alpha \frac{\cos\theta}{\sin\psi} \tag{9}$$

Substitution of Eq. (9) into Eq. (7) gives the radial velocity component in the deformation zone II as:

$$\dot{U}_r = -v_o \frac{r_o}{r}\frac{\sin\alpha}{\sin\psi}\cos\theta \tag{10}$$

The full velocity field for the flow of metal in the deformation zone II is given by the three components of velocity in the cylindrical coordinate system as $\dot{U}_r, \dot{U}_\theta$ and $\dot{U}_z$. The three velocity components for the flow of the material in deformation zone II is obtained by invoking volume constancy. Volume constancy in cylindrical coordinate system is defined as:

$$\dot{\varepsilon}_{rr} + \dot{\varepsilon}_{\theta\theta} + \dot{\varepsilon}_{zz} = 0 \tag{11}$$

where $\dot{\varepsilon}_{ii}$ is the normal strain rate component in the *i*-direction. The strain rates components in cylindrical coordinates can be found from

$$\begin{aligned} &\dot{\varepsilon}_{rr} = \frac{\partial \dot{U}_r}{\partial r} \ , \ \dot{\varepsilon}_{\theta\theta} = \frac{1}{r}\frac{\partial \dot{U}_\theta}{\partial \theta} + \frac{\dot{U}_r}{r} \ , \ \dot{\varepsilon}_{zz} = \frac{\partial \dot{U}_z}{\partial z} \ , \\ &\dot{\varepsilon}_{r\theta} = \frac{1}{2}\left(\frac{\partial \dot{U}_\theta}{\partial r} + \frac{1}{r}\frac{\partial \dot{U}_r}{\partial \theta} - \frac{\dot{U}_\theta}{r}\right) \ , \ \dot{\varepsilon}_{\theta z} = \frac{1}{2}\left(\frac{\partial \dot{U}_\theta}{\partial z} + \frac{1}{r}\frac{\partial \dot{U}_z}{\partial \theta}\right) \ , \ \dot{\varepsilon}_{zr} = \frac{1}{2}\left(\frac{\partial \dot{U}_r}{\partial z} + \frac{\partial \dot{U}_z}{\partial r}\right) \end{aligned} \tag{12}$$

For the plane strain rolling process (i.e. $\dot{U}_z = 0$) and a full velocity field is obtained by placing $\dot{U}_r$, from Eq. (10) into Eqs. (11)-(12), solving for $\dot{U}_\theta$ and applying appropriate boundary conditions, $\dot{U}_\theta\big|_{\theta=0} = 0$ for symmetry axis and $\frac{\dot{U}_\theta}{\dot{U}_r}\Big|_{\theta=\psi} = r\frac{\partial \psi}{\partial r}$ for contact surface, we have

$$\dot{U}_r = -v_o \frac{r_o}{r}\frac{\sin\alpha}{\sin\psi}\cos\theta \ , \ \dot{U}_\theta = -v_o \, r_o \frac{\sin\alpha}{\sin\psi}\cot\psi\frac{\partial \psi}{\partial r}\sin\theta \ , \ \dot{U}_z = 0 \tag{13}$$

Based on the developed velocity field, the strain rate field for deformation zone II can be obtained by Eq. (12) as:

$$\begin{aligned} &\dot{\varepsilon}_{rr} = -\dot{\varepsilon}_{\theta\theta} = v_o \frac{r_o}{r^2}\frac{\sin\alpha}{\sin\psi}(1 + r\frac{\partial \psi}{\partial r}\cot\psi)\cos\theta \\ &\dot{\varepsilon}_{r\theta} = \frac{1}{2}v_o \frac{r_o}{r^2}\frac{\sin\alpha}{\sin\psi}[1 - r^2\cot\psi\frac{\partial^2\psi}{\partial r^2} + r^2(1+\cot^2\psi)(\frac{\partial \psi}{\partial r})^2 + \cot^2\psi(\frac{\partial \psi}{\partial r})^2 + r\cot\psi\frac{\partial \psi}{\partial r}]\sin\theta \\ &\dot{\varepsilon}_{zz} = \dot{\varepsilon}_{\theta z} = \dot{\varepsilon}_{zr} = 0 \end{aligned} \tag{14}$$

where $\frac{\partial \psi}{\partial r}$ is given by differentiation of Eq. (4) as:

$$\frac{\partial \psi}{\partial r} = \frac{r - (R + t_f)\sin\psi - \frac{t_f}{\tan\alpha}\cos\psi}{r[(R + t_f)\cos\psi - \frac{t_f}{\tan\alpha}\sin\psi]} \tag{15}$$

With the strain rate field and the velocity field, the standard upper bound method can be implemented. This upper bound method involves calculating the internal power of deformation over the deformation zone volume, calculating the shear power losses over the two surfaces of velocity discontinuity, and the frictional power losses between the material and the roll.

### *2.3 Determination of power terms*

The internal power of deformation is given by

$$\dot{W}_i = \frac{2}{\sqrt{3}}\sigma_0 \int_v \sqrt{\frac{1}{2}\dot{\varepsilon}_{ij}\dot{\varepsilon}_{ij}}\, dV \tag{16}$$

where $\sigma_0$ is the mean flow stress of the material and $dV$ is a differential volume in the deformation zone. The internal power of deformation in zone II, is determined by

$$\dot{W}_i = \frac{2\sigma_0}{\sqrt{3}} \int_{r_f}^{r_o} \int_0^{\psi(r)} \sqrt{\dot{\varepsilon}_{rr}^2 + \dot{\varepsilon}_{r\theta}^2}\; r\, d\theta\, dr \tag{17}$$

where $\sigma_0$ is given as:

$$\sigma_0 = \frac{\int_0^{\bar{\varepsilon}} \bar{\sigma}\, d\bar{\varepsilon}}{\bar{\varepsilon}}, \quad \bar{\varepsilon} = \frac{2}{\sqrt{3}} \ln \frac{t_o}{t_f} \tag{18}$$

The equation for the power loss along a shear surface is

$$\dot{W}_S = \frac{\sigma_0}{\sqrt{3}} \int_S |\Delta v|\, dS \tag{19}$$

where $|\Delta v|$ is the absolute value of the difference between the velocity components tangent to the boundary, $S$ or velocity discontinuity. The velocity discontinuity between the zones is determined using the velocity of the neighboring zone and the direction of motion in each zone as:

$$|\Delta v_1| = v_o\,(1 + r_o \frac{\partial \psi}{\partial r} \cot\alpha) \sin\theta \tag{20}$$

$$|\Delta v_2| = v_o\,(1 + r_o \frac{t_f}{t_o} \frac{\partial \psi}{\partial r} \cot\alpha) \sin\theta \tag{21}$$

At the entrance and the exit shear surfaces, by placing $(\psi = \alpha, r = r_o)$ and $(\psi = \alpha, r = r_f)$ into Eq. (15), it follows, respectively, that

$$r_o \frac{\partial \psi}{\partial r} = \frac{2(t_o - t_f)}{R \sin 2\alpha} - \tan\alpha \tag{22}$$

$$r_f \frac{\partial \psi}{\partial r} = -\tan\alpha \tag{23}$$

Substituting Eqs. (22)-(23) into Eqs. (20)-(21), and then into Eq. (19) and integrating, the shear power losses along surfaces $S_1$ and $S_2$, respectively, become

$$\dot{W}_{S_1} = \frac{\sigma_0}{\sqrt{3}} v_o\, r_o \frac{t_o - t_f}{R} \frac{1 - \cos\alpha}{\sin^2\alpha} \tag{24}$$

$$\dot{W}_{S_2} = 0 \tag{25}$$

The power expended along the contact surface between the rigid roll and the deforming material will be calculated using

$$\dot{W}_f = \frac{\sigma_0}{\sqrt{3}} m \int_S |\Delta v| dS \tag{26}$$

For contact surface $S_3$, the element of area per unit of width is

$$dS = \sqrt{1+(r\frac{\partial \psi}{\partial r})^2}\, dr \tag{27}$$

Amount of velocity discontinuity can be determined by

$$|\Delta v| = |\dot{U}_r \cos\eta + \dot{U}_\theta \sin\eta + R\omega| \tag{28}$$

where $\eta$ is local angle of the contact arc with respect to the local radial velocity component and

$$\cos\eta = \frac{1}{\sqrt{1+(r\frac{\partial \psi}{\partial r})^2}}, \quad \sin\eta = \frac{r\frac{\partial \psi}{\partial r}}{\sqrt{1+(r\frac{\partial \psi}{\partial r})^2}} \tag{29}$$

Placing Eqs. (27)-(29) into Eq. (26), the frictional power loss per unit with of sheet, along contact surface can be determined as:

$$\dot{W}_f = \frac{\sigma_0}{\sqrt{3}} m v_o r_o \int_{r_f}^{r_o} \left| \frac{1}{r}\frac{\sin\alpha}{\tan\psi} + r\frac{\sin\alpha}{\tan\psi}(\frac{\partial \psi}{\partial r})^2 - \frac{R\omega}{v_o r_o}\sqrt{1+(r\frac{\partial \psi}{\partial r})^2} \right| dr \tag{30}$$

*2.4 Position of neutral point*

The relative velocity between the sheet material and the roll is zero at the neutral point. In this point, point *N* in Fig. 1 with radial and angular positions $r_N$ and $\psi_N$, the linear velocity of roll is equal to the material velocity. On the left hand of the point *N*, the roll surface is moving faster than the sheet material, whereas on the right hand of the point *N*, material moves faster than the roll surface. The velocity vector at a point on the roll surface is coinciding with the tangential line passing through neutral point *N*. Since the velocity discontinuity is in the same direction with the tangent of the roll surface, their values are the same in neutral point *N*, then

$$\dot{U}_r \cos\eta + \dot{U}_\theta \sin\eta = -R\omega \tag{31}$$

where $\omega$ is the angular velocity of the roll and $R\omega$ is the linear velocity of a point on the roll surface. Placing $r = r_N, \theta = \psi_N$ into Eq. (13), the velocity components of neutral point *N* can be determined and by substituting them into the above equation and simplification, we have

$$v_o \frac{r_o}{r_N}\frac{\sin\alpha}{\tan\psi_N} + v_o r_o r_N \frac{\sin\alpha}{\tan\psi_N}(\frac{\partial \psi}{\partial r})^2 = R\omega\sqrt{1+(r\frac{\partial \psi}{\partial r})^2} \tag{32}$$

*2.5 The required rolling torque*

The externally supplied power, $J^*$, for flat rolling is

$$J^* = T\,\omega \tag{33}$$

where $T$ is the required rolling torque per unit width of the sheet. By the upper bound model, the externally supplied power is less than or equal to the sum of the powers described in previous sections. If one assumes the equality, then the total power is

$$J^* = \dot{W}_i + \dot{W}_{S_1} + \dot{W}_f \tag{34}$$

*2.6 Roll separating force*

Neglecting the contribution of the horizontal forces, the roll separating force per unit of width is calculated by the following equation [8, 14]

$$F = \frac{J^*}{L\,\omega} \tag{35}$$

where $F, J^*, L$ and $\omega$ are the rolling force, the rolling power calculated by the upper bound solution, the contact length and the angular velocity of roll respectively. The contact length is calculated as:

$$L = \sqrt{2Rt_o r}\ ,\ r = 1 - \frac{t_f}{t_o} \tag{36}$$

where $r$ is the reduction in thickness.

## 3 THE ROLLING PROCESS OF SYMMETRICAL SANDWICH SHEETS

*3.1 Geometric shape of deformation zones*

Fig. 2 shows the arrangement of the sheets and the roll in rolling process of an initially bonded sandwich sheet. An initially sheet, made up two different ductile materials with the mean flow stresses $\sigma_{0i}$ and $\sigma_{0o}$, is considered. The subscripts $o$ and $i$ denote outer and inner layers, respectively. The material starts as a sheet with total thickness $2t_o$ and outer layer thickness $t_{oo}$ and it rolls into a sheet of total thicknesses $2t_f$ and $t_{of}$ for inner layer. Velocity zones are shown in Fig. 2. The process has one symmetry plane, and then, only a half of the sheet is considered. The same velocity fields of the zones I, II and III described in previous section are used for zones Io, IIo and IIIo of outer layer material and the zones Ii, IIi and IIIi of inner layer material, respectively. In zones Io, Ii, IIIo and IIIi the materials are rigid and move as rigid bodies. Before entering the die, each metal moves with the same velocity $v_o$ in the drawing direction; after drawing, each metal moves with the same velocity $v_f$ in the axial direction. Zone IIo and IIi are the deformation regions. In zones IIo and IIi, the velocities of inner layer and outer layer materials can be given by Eq. (13).

From continuity of material the angle $\beta$, shown in Fig. 2, is given by

$$\sin\beta = \frac{t_o - t_{oo}}{t_o}\sin\alpha \tag{37}$$

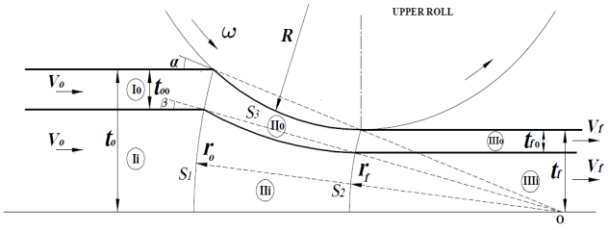


**Fig.2**
Schematic diagram of the rolling of sandwich sheets bonded before rolling and deformation zones.

where $\beta$ is the angle of the line connecting the initial point of the interface surface to the final point of the interface surface with axis of symmetry.

*3.2 Power terms and total power*

The internal power of zones Io, IIIo, Ii, and IIIi, are zero and the equation to calculate the internal power of deformation in zone IIo is

$$\dot{W}_{iIIo} = \frac{2\sigma_{0o}}{\sqrt{3}} \int_{r_f}^{r_o} \int_{\psi_i(r)}^{\psi(r)} \sqrt{\dot{\varepsilon}_{rr}^2 + \dot{\varepsilon}_{r\theta}^2}\; r\, d\theta dr \tag{38}$$

where $\sigma_{0o}$ is the mean flow stress of outer layer material and is determined by

$$\sigma_{0o} = \frac{\int_0^{\bar{\varepsilon}} \bar{\sigma}_o \, d\bar{\varepsilon}}{\bar{\varepsilon}}, \qquad \bar{\varepsilon} = \frac{2}{\sqrt{3}} \ln \frac{t_{oo}}{t_{fo}} \tag{39}$$

and $\psi_i(r)$ is the angular position of the interface surface as a function of the radial distance from the origin $O$ and is given by

$$\psi_i(r) = \sin^{-1}\left[\frac{\sin\beta}{\sin\alpha} \sin\psi(r)\right] \tag{40}$$

The general equation to calculate the internal power of deformation in zone IIi is determined as:

$$\dot{W}_{iIIi} = \frac{2\sigma_{0i}}{\sqrt{3}} \int_{r_f}^{r_o} \int_{0}^{\psi_i(r)} \sqrt{\dot{\varepsilon}_{rr}^2 + \dot{\varepsilon}_{r\theta}^2}\; r\, d\theta dr \tag{41}$$

where $\sigma_{oi}$ is the mean flow stress of the inner layer material and is determined as:

$$\sigma_{0i} = \frac{\int_0^{\bar{\varepsilon}} \bar{\sigma}_i \, d\bar{\varepsilon}}{\bar{\varepsilon}}, \qquad \bar{\varepsilon} = \frac{2}{\sqrt{3}} \ln \frac{t_o - t_{oo}}{t_f - t_{fo}} \tag{42}$$

The shear power consumed along shear boundary $S_1$ can be split up into two parts as:

$$\dot{W}_{S_{1i}} = \frac{\sigma_{0i}}{\sqrt{3}} v_o\, r_o \frac{t_o - t_f}{R} \frac{1-\cos\beta}{\sin^2\alpha} \tag{43}$$

$$\dot{W}_{S_{1o}} = \frac{\sigma_{0o}}{\sqrt{3}} v_o\, r_o \frac{t_o - t_f}{R} \frac{\cos\beta - \cos\alpha}{\sin^2\alpha} \tag{44}$$

The frictional power loss along the contact surface, is calculated by Eq. (25) by placing $\sigma_{0o}$ instead of $\sigma_0$. The total upper bound solution for rolling torque is given by

$$T = \frac{\dot{W}_{iIIo} + \dot{W}_{iIIi} + \dot{W}_{S_{1o}} + \dot{W}_{S_{1i}} + \dot{W}_f}{\omega} \tag{45}$$

## 4 RESULTS AND DISCUSSION

### *4.1 Single layer sheet rolling*

In order to verify the validity of the upper bound approach for flat rolling process, presented in the previous sections, results obtained from the theoretical model are compared with available experimental of data of Ref. [15] as well as with the finite element simulations results. The calculation has been carried out under various rolling conditions, geometrical data and mechanical properties utilized in the rolling analysis are summarized in Table 1. During theoretical analysis and numerical simulations, *m* is set at 0.3 for the contact surface between the roll and sheet.

**Table 1**
Geometrical data and mechanical properties used for computations.

| Case | $t_o$ (*mm*) | $t_f$ (*mm*) | Reduction |
|---|---|---|---|
| 1 | 6.274 | 5.385 | 14.17 |
| 2 | 6.274 | 4.902 | 21.86 |
| 3 | 6.274 | 4.445 | 29.40 |
| 4 | 6.274 | 4.115 | 34.41 |

Radius of the rolls, R=79.375 (*mm*)

Material: Aluminum $\bar{\sigma} = 50.3(1 + \frac{\bar{\varepsilon}}{0.05})^{0.26}$

#### *4.1.1 Numerical Simulation*

The FEM simulations are conducted on the available commercial explicit/FEM software, ABAQUS, to verify the analytical model and study the effects of upper bond method assumptions on the obtained results. Due to the symmetry of the process, the finite element meshes are generated on the upper half cross-section of the sheet. The sheet is meshed by 2D plane strain, linear, four-noded CPE4R elements. The sheet model contains 2700 elements. In this model, the rolls are modeled as rigid bodies. The rolls are rotated by constant angular velocity of $\omega = 201.6 \text{rad/s}$ about their axes. For verification of theoretical study, the results of the rolling torque and the rolling force are extracted from FEM simulations.

#### *4.1.2 Rolling torque and roll separating force*

The comparisons between the computed results and the experimental values for the rolling torque and roll separating force as a function of the rolling reduction are shown in Figs. 3 and 4, respectively. It is observed

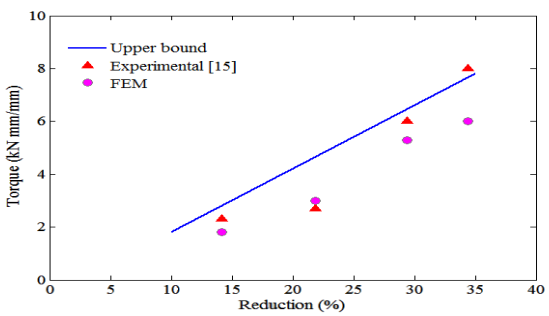


**Fig.3**
Comparison of analytical, FEM and experimental roll torque (per unit of width) as a function of the percentage of reduction.

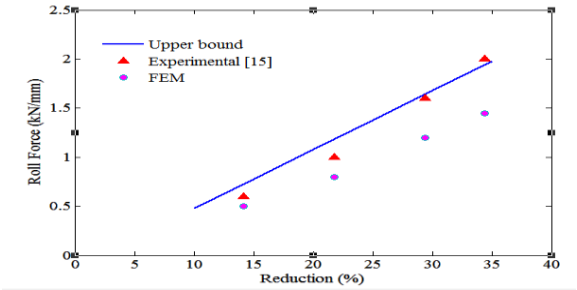


**Fig.4**
Comparison of analytical, FEM and experimental roll separating force (per unit of width) as a function of the percentage of reduction.

That the proposed velocity field leads to a computationally efficient procedure which gives good agreement with experimental data. From Figs. 3 and 4, it can be seen that the calculated forces and torques are basically in agreement with the measured ones. As expected, the predicted rolling torques and forces are always greater than the experimental and FEM results, because the present theoretical values are upper bound solutions. As it can be seen the FEM results for the torque and force are smaller than the measured values. The reason for such discrepancies may be attributed to the assumption of rigid rolls as well as to difficulties in modeling friction in the contact surface between the rolls and the deforming sheet. It can be checked from Figs. 3 and 4 that both rolling force and torque increase with increase in reduction.

*4.2 Sandwich sheet rolling*

To test the validity of the present approach for the rolling of symmetrical sandwich sheets, results obtained from the theoretical model are compared with the finite element simulations results. Four combinations of sandwich sheets St/Al/St are tested. Geometric data utilized in the analysis are summarized in Table 2. Friction factor 0.3 is considered for contact surface between the sheet and the rigid roll. The flow stresses for copper and aluminum in room temperature are obtained as [12]

$$\bar{\sigma} = 212\,(\bar{\varepsilon})^{0.21}\ \text{MPa for purealuminum}\left(\text{Al1100}\right) \tag{46}$$

$$\bar{\sigma} = 552(\,\bar{\varepsilon})^{0.4}\ \text{MPa for mild steel}\ \left(\text{St12}\right) \tag{47}$$

**Table 2**
Geometric data and mechanical properties used for computations.

| Case | $t_o\ (mm)$ | $t_{oo}\ (mm)$ | $t_f\ (mm)$ | Reduction |
|---|---|---|---|---|
| 1 | 6.274 | 2 | 5.385 | 14.17 |
| 2 | 6.274 | 2 | 4.902 | 21.86 |
| 3 | 6.274 | 2 | 4.445 | 29.40 |
| 4 | 6.274 | 2 | 4.115 | 34.41 |

The comparison between the computed results and the FEM values for the rolling torque as a function of the rolling reduction is shown in Fig. 5. It can be seen that the calculated forces and torques by Eq. (45) are basically in agreement with the FEM ones; their average errors are no more than 20%. In addition, it should be noted that further validation with experimental data, is also need to be carried out in the future.

The relation between the FEM and theoretically predicted values of the final thickness of each layer can also be assessed. Analytical predictions of final thickness of outer layer for different reductions are compared with the FEM results in Table 3. This table reveals that the close agreement existing between the two sets of results.

**Table 3**
Comparing the thickness of outer layer $t_{fo}$ with FEM results.

| Case | Initial thickness | Analytical prediction (*mm*) | FEM prediction (*mm*) |
|---|---|---|---|
| 1 | 2 | 1.7164 | 1.68 |
| 2 | 2 | 1.5628 | 1.52 |
| 3 | 2 | 1.4120 | 1.33 |
| 4 | 2 | 1.3118 | 1.26 |

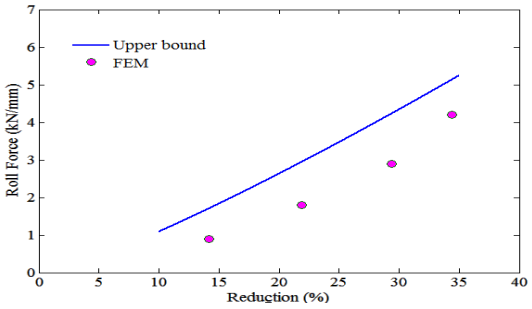


**Fig.5**
Comparison of analytical and FEM roll separating force (per unit of width) as a function of the percentage of reduction for sandwich sheet rolling.

## 5 CONCLUSIONS

(1) A kinematically admissible velocity field for use in upper bound analysis of flat rolling process was developed.
(2) Equations for the strain rate field, power dissipation within the plastic deformation zone, at the velocity discontinuities and at the friction surface have been developed in terms of ordinary integrals. These allow the calculation of the total power required for the rolling process.
(3) The theoretical predictions of rolling torque, rolling force and final thicknesses of the sheet are found to be in good agreement with those obtained by FEM simulations.
(4) With attention to the good agreement between the analytical and FEM results, the mathematical model is capable to assess the rolling of symmetrical sandwich sheet and is able to offer useful knowledge in manufacturing the sandwich sheets with certain thickness of each layer.

## REFERENCES

[1] Avitzur B., Pachla W., 1986, The upper bound approach to plane strain problems using linear and rotational velocity fields-part I: Basic concepts, *Journal of Engineering for Industry* **108**: 295-306.
[2] Avitzur B., Pachla W., 1986, The upper bound approach to plane strain problems using linear and rotational velocity fields- part II: Application, *Journal of Engineering for Industry* **108**: 307-316.
[3] Hwang Y.M., Chen T.H., Hsu H.S., 1996, Analysis of asymmetrical clad sheet rolling by stream function method, *International Journal of Mechanical Sciences* **38**: 443-460.
[4] Hwang Y.M., Hsu H.H., Lee H.J., 1996, Analysis of plastic instability during sandwich sheet rolling, *International Journal of Machine Tools and Manufacture* **36**: 47-62.
[5] Hwang Y.M., Hsu H.H., Lee H.J., 1995, Analysis of sandwich sheet rolling by stream function method, *International Journal of Mechanical Sciences* **37**: 297-315.
[6] Hwang Y.M., Hsu H.H., Hwang Y.L., 2000, Analytical and experimental study on bonding behavior at the roll gap during complex rolling of sandwich sheets, *International Journal of Mechanical Sciences* **42**: 2417-2437.
[7] Martins P.A.F., Manuel Barata Marques M.J., 1999, Upper bound analysis of plane strain rolling using a flow function and the weighted residuals method, *International Journal for Numerical Methods in Engineering* **44**: 1671-1683.
[8] Dogruoglu A.N., 2001, On constructing kinematically admissible velocity fields in cold sheet rolling, *Journal of Materials Processing Technology* **110**: 287-299.
[9] Maleki H., Bagherzadeh S., Mollaei-Dariani B., Abrinia K., 2013, Analysis of bonding behavior and critical reduction of two-layer strips in clad cold rolling process, *Journal of Materials Engineering and Performance* **22**: 917-925.
[10] Zhang S., Song B., Wang X., Zhao D., 2014, Analysis of plate rolling by MY criterion and global weighted velocity field, *Applied Mathematical Modelling* **38**: 3485-3494.
[11] Hwang Y.M., Kiuchi M., 1992, Analysis of asymmetrical complex rolling of multi-layer sheet by upper bound method, *The Journal of the Chinese Society of Mechanical Engineers* **13**: 33-45.
[12] Al Salehi F.A., Firbank T.C., Lancaster P.G., 1973, An experimental determination of the roll pressure distributions in cold rolling, *International Journal of Mechanical Sciences* **15**: 693-700.